Computation of reflector surfaces for two-variable beam shaping in the hyperbolic case

1976 J. Phys. A: Math. Gen. 9 611

(http://iopscience.iop.org/0305-4470/9/4/018)

J. Phys. A: Math. Gen., Vol. 9, No. 4, 1976. Printed in Great Britain.

Computation of reflector surfaces for two-variable beam shaping in the hyperbolic case

B S Westcott and F Brickell

Mathematics Department, Southampton University, Southampton SO9 5NH, UK

Received 3 November 1975

Abstract. Previous work on the hyperbolic case has shown that the synthesis of a reflector surface under the geometric-optics approximation, given feed and far-field power patterns, can be formulated as an initial-value problem involving the solution of a set of simultaneous quasi-linear first-order partial differential equations. A numerical method of solution is proposed in this paper based on finite differences and is tested against exact solutions. Examples of reflector surfaces so generated are illustrated.

1. Introduction

The problem of synthesizing a reflector surface capable of producing a two-variable generalized far-field pattern when illuminated by a point source has been considered in several recent papers under the geometric-optics approximation.

Mathematically the problem can be formulated in terms of either nonlinear or quasi-linear partial differential equations. Thus Westcott and Norris (1975) show that the elliptic case can be solved under certain conditions as a nonlinear boundary-value problem involving a second-order partial differential equation of the Monge–Ampère type.

An alternative treatment proposed by Brickell and Westcott (1976, to be referred to as I), generates a set of nonlinear partial differential equations of the first order which, in the spherical coordinates of figure 1, may be written

$$A\alpha_\theta + B\alpha_\phi + C\beta_\theta + E\beta_\phi = 0 \tag{1}$$

$$\alpha_\theta\beta_\phi - \alpha_\phi\beta_\theta = \pm D \sin\theta/\sin\alpha \tag{2}$$

with α, β denoting incident ray direction and θ, ϕ denoting reflected ray direction; A, B, C, E are functions of $\alpha, \beta, \theta, \phi$ and $D(\alpha, \beta, \theta, \phi)$ is the ratio G/I between the given reflected far-field power density $G(\theta, \phi)$ and the incident power density $I(\alpha, \beta)$. The set of equations is hyperbolic or elliptic accordingly as the + or − sign is chosen in (2).

In this paper we consider the hyperbolic case and to obtain numerical solutions we prefer not to deal with the set (1) and (2) but to use a derived set of quasi-linear equations obtained in I by a method related to the method of characteristics.

These equations are presented in § 2 and the choice of initial conditions for their solution is discussed in § 3. The finite-difference formulae for these solutions are

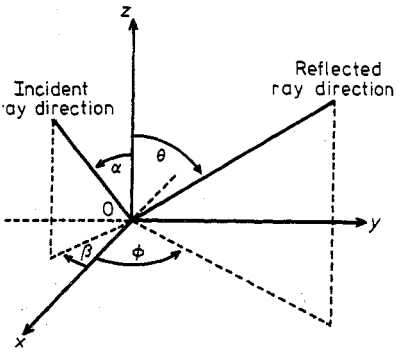

Figure 1. Diagram showing coordinate system.

derived in § 4. Analytical test models which evidence the accuracy of the procedure appear in § 5 and § 6 contains results for two more practical models. The final section (§ 7) contains our conclusions.

2. The equations

We have shown previously in I that in order to carry out the solution it is convenient to regard $\alpha, \beta, \theta, \phi$ as functions of new independent variables (x, y) closely related to the characteristics of the hyperbolic system. It can be shown that, by using these variables, equations (1) and (2) are replaced by a quasi-linear set of four simultaneous equations for the unknown functions $\alpha, \beta, \theta, \phi$, namely

$$\begin{aligned} A\frac{\partial\alpha}{\partial x}+C\frac{\partial\beta}{\partial x}&=-\Delta\frac{\partial\theta}{\partial y},\\ B\frac{\partial\alpha}{\partial x}+E\frac{\partial\beta}{\partial x}&=-\Delta\frac{\partial\phi}{\partial y},\\ A\frac{\partial\alpha}{\partial y}+C\frac{\partial\beta}{\partial y}&=-\Delta\frac{\partial\theta}{\partial x},\\ B\frac{\partial\alpha}{\partial y}+E\frac{\partial\beta}{\partial y}&=-\Delta\frac{\partial\phi}{\partial x}, \end{aligned} \tag{3}$$

where

$$\Delta=[(BC-AE)D\sin\theta/\sin\alpha]^{1/2}$$

and

$$\begin{aligned} A&=\sin\theta(\cos\alpha-\cos\theta)\sin(\beta-\phi)\\ B&=(1-\cos\theta\cos\alpha)\cos(\beta-\phi)-\sin\theta\sin\alpha\\ C&=\sin\alpha\sin\theta B\\ E&=\sin\alpha(\cos\theta-\cos\alpha)\sin(\beta-\phi). \end{aligned}$$

Hence

$$BC-AE=\Lambda^2 \sin\theta \sin\alpha,$$

where

$$\Lambda=1-\sin\alpha \sin\theta \cos(\beta-\phi)-\cos\alpha \cos\theta$$

and $\Delta=D^{1/2}\Lambda \sin\theta$ is real and positive.

The reflector surface $r(\theta, \phi)$ may be developed from a solution of (3) by first integrating the equations derived in I from the geometrical law of reflection, i.e.

$$\sigma_\theta=-(\tilde{X}\alpha_\theta+\tilde{Y}\beta_\theta)/\Lambda \tag{4}$$

$$\sigma_\phi=-(\tilde{X}\alpha_\phi+\tilde{Y}\beta_\phi)/\Lambda \tag{5}$$

where

$$\tilde{X}=\sin\alpha \cos\theta-\sin\theta \cos\alpha \cos(\beta-\phi)$$

$$\tilde{Y}=\sin\alpha \sin\theta \sin(\beta-\phi)$$

and then putting $r(\theta, \phi)=\exp(\sigma(\theta, \phi))$.

The characteristics of the system (3) are $y=\pm x+$constant so that $y=0$ is *not* a characteristic. Consequently standard theory (see, e.g., Courant and Hilbert 1962) implies that there are unique solutions of (3) such that $\alpha, \beta, \theta, \phi$ are prescribed functions on $y=0$. Provided that the Jacobian determinant

$$J=\begin{vmatrix}\theta_x & \theta_y\\ \phi_x & \phi_y\end{vmatrix}$$

does not vanish on the line $y=0$, we can express α, β as functions of θ, ϕ. It is shown in I that these functions satisfy the equations (1) and (2) (with the + sign). By using the equations (3) the condition on J is easily shown to be the same as

$$(A\alpha_x+C\beta_x)\phi_x-(B\alpha_x+E\beta_x)\theta_x\neq 0 \tag{6}$$

on the line $y=0$.

3. Initial conditions

The initial conditions on $\alpha, \beta, \theta, \phi$ are of course arbitrary, subject to the above condition on the Jacobian. On $y=0$ we assume $\alpha=\pi/2, \beta=f(x), \theta=\pi/2, \phi=x$ where $f(x)$ is for the moment arbitrary. Physically this means that a reflector is designed so that initially a given curve l of reflected ray directions defined by $\theta=\pi/2, \phi=x$ arises from a given curve L of incident ray directions $\alpha=\pi/2, \beta=f(x)$. Thus both initial curves l, L lie in the $Z=0$ plane of the spherical coordinate system.

From the definitions of A, B, C, E we find that $A=E=0, B=C=\cos(f(x)-x)-1$ and hence (6) becomes

$$[1-\cos(f(x)-x)]f'(x)\neq 0. \tag{7}$$

The choice of $f(x)$ is decided by the following considerations. On the curve l

$$\partial\alpha/\partial\phi=0, \qquad \partial\beta/\partial\theta=0 \qquad \text{(from(1))}$$

$$\partial\beta/\partial\phi=f'(x), \qquad \partial\alpha/\partial\theta=D/f'(x) \qquad \text{(from(2))}.$$

Now the values of $\partial\beta/\partial\phi$, $\partial\alpha/\partial\theta$ are the respective factors by which tangential vectors to the unit sphere in the direction of l and perpendicular to the direction of l are stretched. In this paper we shall keep these distortions the same by choosing $\mathrm{d}f/\mathrm{d}x = D^{1/2}$ although, in some applications, it may be advantageous to use unequal distortions of the initial vectors. It follows that the equation

$$\int (I(\pi/2, f))^{1/2}\,\mathrm{d}f = \int (G(\pi/2, x))^{1/2}\,\mathrm{d}x$$

must be solved for $f(x)$. Our examples have been chosen to give explicit analytic solutions for $f(x)$ but in general it is sufficient only to obtain $f(x)$ numerically over the prescribed range of x.

The function f can still be altered by an additive constant. We fix this constant by choosing a value for $f(\pi/2)$ within the interval $(-\pi/2, 0)$. The precise choice is governed by the condition that, to avoid source blockage in the plane $Z = 0$,

$$0 < x - f(x) < \pi$$

for the range of values of x under consideration.

The value of $\sigma(x, 0) = \tau(x)$ is determined by the initial conditions. From (4), (5)

$$\sigma_\alpha = -\tilde{X}/\Lambda, \qquad \sigma_\beta = -\tilde{Y}/\Lambda.$$

On the curve $y = 0$ we have

$$\tilde{X} = 0, \qquad \tilde{Y} = \sin(f(x) - x), \qquad \Lambda = 1 - \cos(f(x) - x)$$

and consequently by the chain rule

$$\frac{\mathrm{d}\tau}{\mathrm{d}x} = \frac{\partial\sigma}{\partial\alpha}0 + \frac{\partial\sigma}{\partial\beta}\frac{\mathrm{d}f}{\mathrm{d}x} = f'(x)\cot[\tfrac{1}{2}(x - f(x))].$$

Then

$$\tau(x) = \int_{\pi/2}^{x} f'(u)\cot[\tfrac{1}{2}(u - f(u))]\,\mathrm{d}u \tag{8}$$

where we have set $\tau(\pi/2) = 0$. Geometrically the function $\tau(x)$ determines the curve of intersection Γ of the reflector with the plane $Z = 0$. In general the integral (8) has to be obtained numerically for values of x within the initial range along $y = 0$.

4. Finite-difference formulae

In this section we shall develop difference formulae for the approximate integration of equations (3), (4), (5). Suppose that the curve l has been limited to an interval $a \leq \phi \leq b$ containing the point $\phi = \pi/2$. Our initial conditions are thus set on the line $y = 0$ between the points $(a, 0)$ and $(b, 0)$. In our examples we have $a = \pi/3$, $b = 2\pi/3$.

We construct a rectangular grid containing the points $(a, 0)$, $(b, 0)$ and with lines parallel to the x and y axes. Let h, k be the grid spacings in the x and y directions respectively with h chosen so that $(b - a) = (2n - 2)h$ where n is a positive integer. In our examples we have chosen $n = 46$.

The base line for the computation is $y = 0$ and we have called this the grid line $j = 1$. The points $(a, 0)$, $(b, 0)$ become the grid points $(1, 1)$, $(2n - 1, 1)$ respectively, and the

initial values of the dependent variables are set at the grid points $(i, 1)$, $i=1,\ldots,2n-1$. At the second level $j=2$ and grid points are taken at $i=2,\ldots,2n-2$; at the third level $j=3$ and $i=3,\ldots,2n-3$ and so on until $j=n$ and $i=n$. We shall compute the dependent variables at these grid points. They lie in a triangular region in $y \geqslant 0$.

It is known from general theory that a solution of (3) is uniquely determined by the initial conditions only within the square formed by the characteristics $y=\pm(x-a)$, $y=\pm(x-b)$. It is therefore essential to choose $k \leqslant h$ so that our triangular region lies within this square.

First of all we shall develop first-order difference formulae. In practice we have found that these formulae may only give good results near the initial line. Consequently, in this paper, we use them only to compute the solutions along the second level, $j=2$, in terms of the initial values along $j=1$. For higher levels, $j>2$, second-order differences are used to compute the solutions in terms of the values along the two previous levels, $j-1, j-2$.

It is convenient to use matrix notation. We write the system (3) as

$$\mathbf{u}_x + \mathbf{K}\mathbf{v}_y = 0 \tag{9}$$

$$\mathbf{u}_y + \mathbf{K}\mathbf{v}_x = 0 \tag{10}$$

where

$$\mathbf{u} = \begin{pmatrix} \theta \\ \phi \end{pmatrix}, \qquad \mathbf{v} = \begin{pmatrix} \alpha \\ \beta \end{pmatrix}, \qquad \mathbf{K} = \Delta^{-1} \begin{pmatrix} A & C \\ B & E \end{pmatrix}.$$

We recall that $\mathbf{K}$ is a function of the dependent variables $\mathbf{u}$, $\mathbf{v}$ only.

4.1. *First-order difference formulae*

We add and subtract (9), (10) to obtain

$$\mathrm{D}_1\mathbf{u} + \mathbf{K}\mathrm{D}_1\mathbf{v} = 0 \tag{11}$$

$$\mathrm{D}_2\mathbf{u} - \mathbf{K}\mathrm{D}_2\mathbf{v} = 0 \tag{12}$$

where $\mathrm{D}_1 \equiv \partial/\partial x + \partial/\partial y$, $\mathrm{D}_2 \equiv \partial/\partial y - \partial/\partial x$ are the derivatives in the directions of the characteristics.

Following the method given in Forsythe and Wasow (1960) we obtain our difference equations from the equations (11) and (12). Consider the grid points

$$\mathrm{P}(ih, (j+1)k),$$

$$\mathrm{R}((i-1)h, jk), \qquad \mathrm{S}(ih, jk), \qquad \mathrm{T}((i+1)h, jk)$$

and define first-order differences in the forward and backward x directions at S by

$$\Delta_x \mathbf{u}_\mathrm{S} = \mathbf{u}_\mathrm{T} - \mathbf{u}_\mathrm{S}, \qquad \nabla_x \mathbf{u}_\mathrm{S} = \mathbf{u}_\mathrm{S} - \mathbf{u}_\mathrm{R}$$

respectively. Now use backward differences for $\partial/\partial x$ in (11), forward differences for $\partial/\partial x$ in (12), and forward differences for $\partial/\partial y$ in both equations. It follows that, correct to first order,

$$\gamma\nabla_x \mathbf{u}_\mathrm{S} + \Delta_y \mathbf{u}_\mathrm{S} + \mathbf{K}_\mathrm{S}(\gamma\nabla_x \mathbf{v}_\mathrm{S} + \Delta_y \mathbf{v}_\mathrm{S}) = 0 \tag{13}$$

$$\Delta_y \mathbf{u}_\mathrm{S} - \gamma\Delta_x \mathbf{u}_\mathrm{S} - \mathbf{K}_\mathrm{S}(\Delta_y \mathbf{v}_\mathrm{S} - \gamma\Delta_x \mathbf{v}_\mathrm{S}) = 0 \tag{14}$$

where $\gamma = k/h$ is the grid ratio and $\mathbf{K}_\mathrm{S}$ denotes the value of the matrix $\mathbf{K}$ at the point S.

Adding and subtracting (13), (14) we obtain

$$\Delta_y \mathbf{u}_S = \tfrac{1}{2}\gamma[(\Delta_x - \nabla_x)\mathbf{u}_S - \mathbf{K}_S(\nabla_x + \Delta_x)\mathbf{v}_S],$$
$$\Delta_y \mathbf{v}_S = \tfrac{1}{2}\gamma[(\Delta_x - \nabla_x)\mathbf{v}_S - \mathbf{K}_S^{-1}(\nabla_x + \Delta_x)\mathbf{u}_S]$$

and we write these equations as

$$\mathbf{u}_P = \mathbf{u}_S + \tfrac{1}{2}\gamma[(\Delta_x - \nabla_x)\mathbf{u}_S - \mathbf{K}_S(\nabla_x + \Delta_x)\mathbf{v}_S], \tag{15}$$
$$\mathbf{v}_P = \mathbf{v}_S + \tfrac{1}{2}\gamma[(\Delta_x - \nabla_x)\mathbf{v}_S - \mathbf{K}_S^{-1}(\nabla_x + \Delta_x)\mathbf{u}_S]. \tag{16}$$

The equations (15), (16) are our first-order difference formulae for the dependent variables $\mathbf{u}, \mathbf{v}$.

We shall develop a first-order formula for the variable σ in a similar way. We have from (4), (5)

$$\sigma_\alpha = L, \qquad \sigma_\beta = M \tag{17}$$

where $L = -\tilde{X}/\Lambda$, $M = -\tilde{Y}/\Lambda$. The derivatives $D_1\sigma, D_2\sigma$ are given by

$$D_1\sigma = LD_1\alpha + MD_1\beta, \qquad D_2\sigma = LD_2\alpha + MD_2\beta$$

and first-order approximations to these equations are

$$\gamma\nabla_x\sigma_S + \Delta_y\sigma_S = L_S(\gamma\nabla_x\alpha_S + \Delta_y\alpha_S) + M_S(\gamma\nabla_x\beta_S + \Delta_y\beta_S),$$
$$-\gamma\Delta_x\sigma_S + \Delta_y\sigma_S = L_S(-\gamma\Delta_x\alpha_S + \Delta_y\alpha_S) + M_S(-\gamma\Delta_x\beta_S + \Delta_y\beta_S).$$

We obtain our difference formula for σ by adding the above equations. We find

$$2\Delta_y\sigma_S + \gamma(\nabla_x - \Delta_x)\sigma_S = L_S[\gamma(\nabla_x - \Delta_x) + 2\Delta_y]\alpha_S + M_S[\gamma(\nabla_x - \Delta_x) + 2\Delta_y]\beta_S$$

and we write this equation as

$$\sigma_P = \sigma_S - \tfrac{1}{2}\gamma(\nabla_x - \Delta_x)\sigma_S + \tfrac{1}{2}L_S[\gamma(\nabla_x - \Delta_x) + 2\Delta_y]\alpha_S + \tfrac{1}{2}M_S[\gamma(\nabla_x - \Delta_x) + 2\Delta_y]\beta_S \tag{18}$$

where, of course, $\Delta_y\alpha_S$, $\Delta_y\beta_S$ are given by (16).

As we have explained, equations (15), (16), (18) are used to compute the solutions at level $j = 2$ from the initial values along $j = 1$.

4.2. *Second-order difference formulae*

The computation of the solutions at levels $j > 2$ is achieved by using an explicit formula of Lax–Wendroff type. Consider the seven grid points

	$N(ih, (j+2)k)$,	
$O((i-1)h, (j+1)k)$,	$P(ih, (j+1)k)$,	$Q((i+1)h, (j+1)k)$.
$R((i-1)h, jk)$,	$S(ih, jk)$,	$T((i+1)h, jk)$.

The Lax–Wendroff method (see, e.g., Mitchell 1969) applied to our system (9), (10) ultimately produces

$$\mathbf{u}_N = \mathbf{u}_S - \gamma\mathbf{K}_P(\nabla_x + \Delta_x)\mathbf{v}_S + \gamma^2\mathbf{K}_P[(\mathbf{K}_P^{-1} + \mathbf{K}_Q^{-1})\Delta_x - (\mathbf{K}_O^{-1} + \mathbf{K}_P^{-1})\nabla_x]\mathbf{u}_S, \tag{19}$$
$$\mathbf{v}_N = \mathbf{v}_S - \gamma\mathbf{K}_P^{-1}(\nabla_x + \Delta_x)\mathbf{u}_S + \gamma^2\mathbf{K}_P^{-1}[(\mathbf{K}_P + \mathbf{K}_Q)\Delta_x - (\mathbf{K}_O + \mathbf{K}_P)\nabla_x]\mathbf{v}_S, \tag{20}$$

where $\nabla_x\mathbf{u}_S = \mathbf{u}_S - \mathbf{u}_R$, $\Delta_x\mathbf{u}_S = \mathbf{u}_T - \mathbf{u}_S$ with similar definitions for $\nabla_x\mathbf{v}_S, \Delta_x\mathbf{v}_S$. These formulae are correct to second order.

We have found that the formulae (19), (20) give good results. One has to choose n sufficiently large and $\gamma = k/h$ sufficiently small. For example, in our computations over various models we used $n = 46$ and the chosen values of γ ranged between 0·4 and 1·0. In our computer program both γ and n are input parameters.

The second-order formula for σ is developed *ab initio* as follows:

$$\sigma_N = (\sigma + 2k\sigma_y + 2k^2\sigma_{yy})_S$$
$$= \left[\sigma + 2k(\alpha_y L + \beta_y M) + 2k^2(\alpha_{yy}L + \beta_{yy}M) + 2k^2\left(\alpha_y\frac{\partial L}{\partial y} + \beta_y\frac{\partial M}{\partial y}\right)\right]_S.$$

We can substitute

$$(2k\alpha_y + 2k^2\alpha_{yy})_S = \alpha_N - \alpha_S,$$
$$(2k\beta_y + 2k^2\beta_{yy})_S = \beta_N - \beta_S,$$

where the right-hand sides of both these equations are already evaluated by (20). Furthermore it can be shown by differentiating (17) that

$$\partial L/\partial y = P_1\alpha_y + P_2\beta_y + P_3\theta_y + P_4\phi_y,$$
$$\partial M/\partial y = Q_1\alpha_y + Q_2\beta_y + Q_3\theta_y + Q_4\phi_y,$$

where

$$P_1 = \partial L/\partial\alpha = [\Lambda - \sin^2\theta\,\sin^2(\beta - \phi)]/\Lambda^2, \qquad P_2 = \partial L/\partial\beta = -A/\Lambda^2,$$
$$P_3 = \partial L/\partial\theta = -B/\Lambda^2, \qquad P_4 = \partial L/\partial\phi = A/\Lambda^2,$$
$$Q_1 = \partial M/\partial\alpha = -A/\Lambda^2, \qquad Q_2 = \partial M/\partial\beta = -C/\Lambda^2,$$
$$Q_3 = \partial M/\partial\theta = -E/\Lambda^2, \qquad Q_4 = \partial M/\partial\phi = C/\Lambda^2.$$

Hence

$$\sigma_N = \sigma_S + (\alpha_N - \alpha_S)L_S + (\beta_N - \beta_S)M_S + 2[\Delta_y\alpha_S(P_{1S}\Delta_y\alpha_S + P_{2S}\Delta_y\beta_S + P_{3S}\Delta_y\theta_S + P_{4S}\Delta_y\phi_S)$$
$$+ \Delta_y\beta_S(Q_{1S}\Delta_y\alpha_S + Q_{2S}\Delta_y\beta_S + Q_{3S}\Delta_y\theta_S + Q_{4S}\Delta_y\phi_S)]. \qquad (21)$$

The accuracy of our procedure was tested thoroughly against known analytic models. Two particular models are discussed in the next section and in these the agreement obtained was better than one part in 10^5.

4.3. *Extension to image region $y < 0$*

Given initial conditions along $y = 0$ we have described a method for computing the solutions to the equations (9), (10), (4), (5) in the region $y > 0$. We now explain a simple device which we use to compute the solutions in the region $y < 0$.

We define functions $\bar{\mathbf{u}}$, $\bar{\mathbf{v}}$, $\bar{\sigma}$ by

$$\bar{\mathbf{u}}(x, y) = \mathbf{u}(x, -y),\ \bar{\mathbf{v}}(x, y) = \mathbf{v}(x, -y),\ \bar{\sigma}(x, y) = \sigma(x, -y).$$

It can be shown that these functions satisfy the partial differential equations

$$\frac{\partial\bar{\mathbf{u}}}{\partial x} - \mathbf{K}(\bar{\mathbf{u}}, \bar{\mathbf{v}})\frac{\partial\bar{\mathbf{v}}}{\partial y} = 0, \qquad (22)$$

$$\frac{\partial\bar{\mathbf{u}}}{\partial y} - \mathbf{K}(\bar{\mathbf{u}}, \bar{\mathbf{v}})\frac{\partial\bar{\mathbf{v}}}{\partial x} = 0, \qquad (23)$$

$$\partial\bar{\sigma}/\partial\bar{\alpha} = L(\bar{\mathbf{u}}, \bar{\mathbf{v}}), \qquad \partial\bar{\sigma}/\partial\bar{\beta} = M(\bar{\mathbf{u}}, \bar{\mathbf{v}}). \qquad (24)$$

Obviously the functions $\bar{\mathbf{u}}, \bar{\mathbf{v}}, \bar{\sigma}$ satisfy the same initial conditions as $\mathbf{u}, \mathbf{v}, \sigma$. Consequently all we have to do in order to compute $\mathbf{u}, \mathbf{v}, \sigma$ for negative values of y is to replace the matrix function $\mathbf{K}$ by $-\mathbf{K}$ and repeat the program.

The proof of the equations (22), (23), (24) is an exercise in partial differentiation. We are content to justify equation (22) only. We know from equation (9) that

$$\frac{\partial \mathbf{u}}{\partial x}(x,-y)+\mathbf{K}(\mathbf{u}(x,-y),\mathbf{v}(x,-y))\frac{\partial \mathbf{v}}{\partial y}(x,-y)=0,$$

and (22) is an immediate consequence because

$$\frac{\partial \bar{\mathbf{u}}}{\partial x}(x,y)=\frac{\partial \mathbf{u}}{\partial x}(x,-y), \qquad \frac{\partial \bar{\mathbf{v}}}{\partial y}(x,y)=-\frac{\partial \mathbf{v}}{\partial y}(x,-y).$$

5. Analytic models

In certain cases the nonlinear system of (1), (2) can be solved analytically by separation of variables and we have found them useful in testing the accuracy of our computer programs. We have derived exact solutions in a previous paper and here we are content to quote results in two particular cases.

Model 1. $\alpha = 2\tan^{-1}(u^k)$, $\beta = k(\phi-\pi/2)-\pi/2$ where $u=\tan\frac{1}{2}\theta$.

This solution of (1) when inserted into (2) yields a ϕ-independent profile, namely

$$D = k^2[u^{k-1}(1+u^2)/(1+u^{2k})]^2$$

which for $k>1$ has a maximum at $\theta=\pi/2 (u=1)$ and monotonically decreases to zero as $\theta \to 0, \pi$.

The reflector surface can be obtained explicitly from (4), (5) and if for simplicity we take $k=2$ then

$$r = 8(1+u^4)/(1+u^2+2u\sin\phi)^2,$$

where $r=1$ when $\theta=\pi/2, \phi=\pi/2$.

To test our program we assumed the following initial conditions:

$$\theta=\alpha=\pi/2, \qquad \phi=x, \qquad \beta=2x-3\pi/2$$

and from (8)

$$\tau(x)=2\ln[2/(1+\sin x)]$$

with x limited to the range $(\pi/3, 2\pi/3)$. We integrated with $\gamma=0{\cdot}6$, $n=46$ and found that this gave us a range of 68° for α; 120° for β; 35° for θ and 60° for ϕ. The agreement between the computed results and the exact formulae was very good (better than one part in 10^5).

Reflector cross sections appear in figure 2. An interesting feature in the vertical cross section ($\beta=-90°$) is that towards the edges the reflector bends away from the direction of the inward normal indicating a saddle-shaped surface. Such behaviour for hyperbolic cases is predicted by the theory on reflector curvature as given in I. The reflector given by this model is not a practical design since it suffers from source blockage in the direction ($\theta=\phi=\pi/2$) of maximum D.

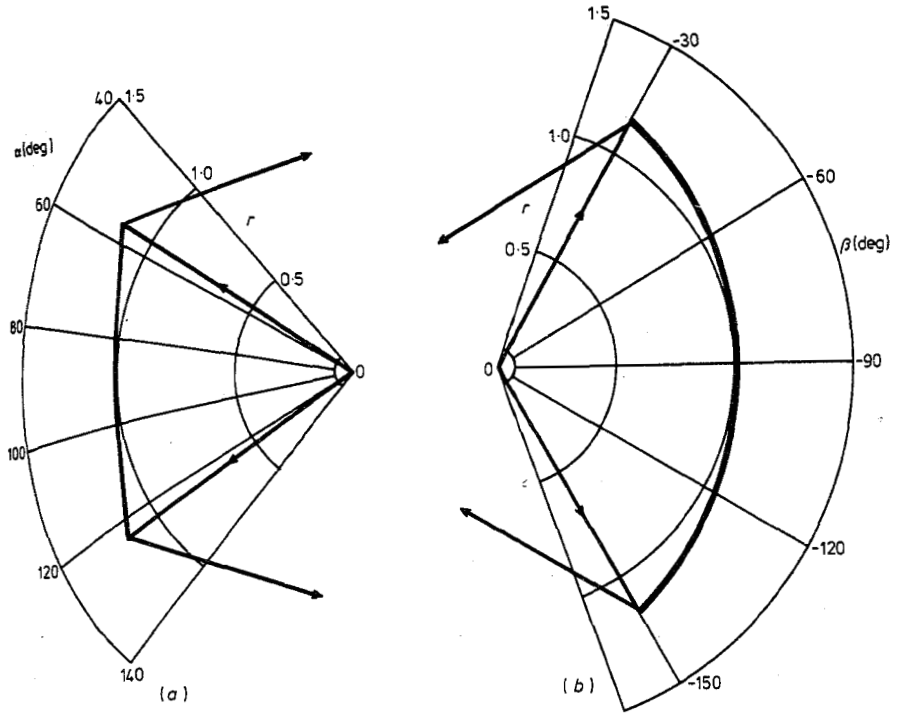

Figure 2. Reflector cross sections for test model 1: (*a*) in $\beta = -\pi/2$ plane showing edge rays; (*b*) in $\alpha = \pi/2$ plane showing edge rays.

Model 2. $\alpha = 2\tan^{-1}(\exp k\phi)$, $\beta = -k\ln(\tan\frac{1}{2}\theta)$ with k arbitrary.

This solution of (1) when inserted into (2) yields

$$D = k^2 \operatorname{sech}^2 k\phi \operatorname{cosec}^2\theta$$

and possesses singularities at $\theta = 0, \pi$. In testing our program we used $k = -1$ and the following initial conditions:

$$\alpha = 2\tan^{-1}(e^{-x}), \qquad \beta = 0, \qquad \theta = \pi/2, \qquad \phi = x$$

and easily derived from (4), (5),

$$\tau(x) = -\int_{\pi/2}^{x} \frac{\tanh u \cos u \, du}{\cosh u - \cos u}$$

evaluated for x over the range $(\pi/3, 2\pi/3)$ by Gaussian quadratures.

An explicit form for the reflector surface is not forthcoming in this case.

Comparison between program results and analytical results was again excellent (better than one part in 10^5) over the whole range of the integration, when the parameter values $\gamma = 0{\cdot}6$, $n = 46$ were used. The values of θ obtained in the integration were within the range (76°, 109°), and hence the singularity was avoided.

The two models considered above although not leading to useful reflector designs provide an invaluable check on the accuracy of the finite-difference formulae. Of these models the second one involving exponential solutions provides a most rigorous test.

We now consider some typical examples in which reasonable reflector surfaces are obtained numerically.

6. Computed reflector surfaces

Model 3. Isotropic source

A reflector is required to produce a far-field

$$G(\theta, \phi) = \frac{16 \sin^2\theta \sin^2\phi}{\cosh^2(8 \cos\theta) \cosh^2(6 \cos\phi)} \tag{25}$$

given that the source illumination is isotropic over the surface of the reflector and normalized to unity (i.e. $I = 1$).

It follows that $D(\theta, \phi) = G(\theta, \phi)$ and contours of constant G are normalized to unity at peak value (when $\theta = \phi = \pi/2$) and plotted in decibels against reflected ray direction (θ, ϕ) in figure 3. It is evident that this model corresponds to an elliptical beam possessing a 3 dB beam width of 13° by 17° in the θ, ϕ directions respectively. The −9 dB contour encloses an elliptical region extending over a range of about 24° in θ and 32° in ϕ.

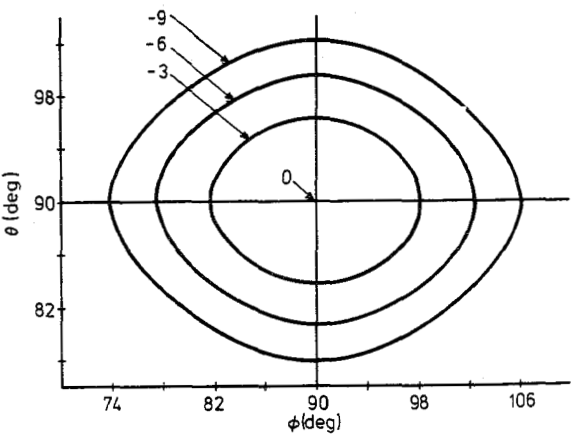

Figure 3. Constant G contours (labelled in decibels) against reflected ray direction for model 3.

Initially, i.e. on $y = 0$, the following conditions are assumed:

$$\theta = \pi/2, \qquad \phi = x, \qquad \alpha = \pi/2, \qquad \beta = f(x), \qquad \pi/3 \leq x \leq 2\pi/3,$$

where $f(x)$ is given by the considerations of § 3.

We have

$$\mathrm{d}f/\mathrm{d}x = (\mathrm{D}(\pi/2, x))^{1/2} = 4 \sin x/\cosh(6 \cos x)$$

so that integrating we obtain

$$f(x) = -\tfrac{4}{3} \tan^{-1}[\exp(6 \cos x)] + \text{constant}.$$

The arbitrary constant is zero if we choose $f(\pi/2) = -\pi/3$ and thereby satisfy the zero blockage condition $0 < x - f(x) < \pi$ for x in $(\pi/3, 2\pi/3)$. Inserting the expression for $f(x)$ into (8) we obtain the integral

$$\tau(x) = 4 \int_{\pi/2}^{x} \frac{\cot\{\frac{1}{2}u + \frac{2}{3}\tan^{-1}[\exp(6\cos u)]\} \sin u \, du}{\cosh(6\cos u)}$$

which is evaluated numerically by Gaussian quadratures in our program.

The results of integrating the partial differential equations (3) were used to obtain G as a function of α, β and contours of constant G are plotted against α, β in figure 4. The -9 dB contour surrounds an elliptical region of the (α, β) plane with a range extending approximately 50° in the α direction and 90° in the β direction. A reflector occupying this solid angle would produce the corresponding solid angle in the reflected field as shown in figure 3.

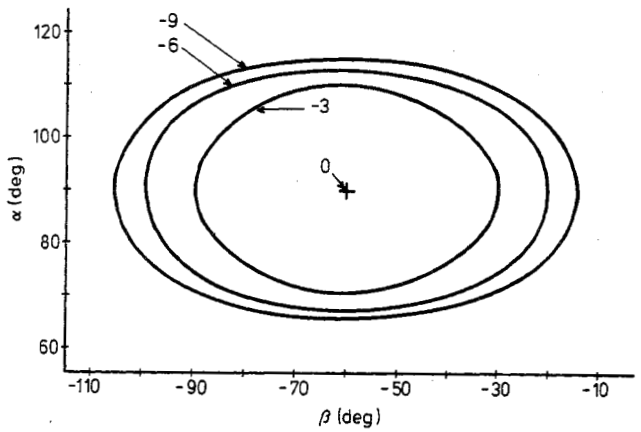

Figure 4. Constant G contours (labelled in decibels) against incident ray direction for model 3.

The subsidiary integration of (4) and (5) for the reflector surface yields the cross sections of figure 5. Edge rays are drawn on the cross section in the $Z = 0$ plane and show that source blockage in this plane is avoided. The vertical cross section in the plane $\beta = -\pi/3$ shows an outward taper towards the edges, typical of reflectors designed by the hyperbolic theory.

Model 4. Tapered feed pattern

We use the above model given by the expression (25) for $G(\theta, \phi)$ but taper the source illumination pattern conically according to the law

$$I(\lambda) = \frac{1}{(1 + \frac{9}{16}\lambda^2)^2} \tag{26}$$

where $\lambda = \lambda(\alpha, \beta)$ is confined to the interval $0 \leq \lambda < \pi/2$.

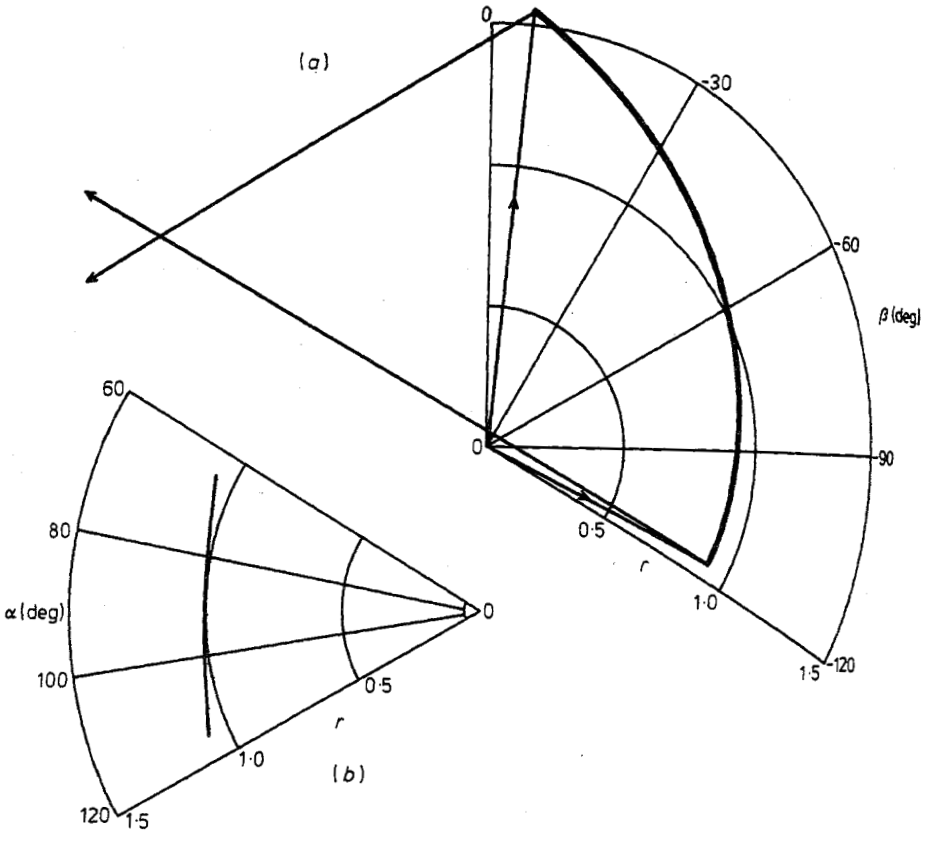

Figure 5. Reflector cross sections for model 3: (*a*) in $\alpha = \pi/2$ plane showing edge rays; (*b*) in $\beta = -\pi/3$ plane.

The axis of the feed pattern and hence the maximum feed illumination is directed along the direction $\alpha = \pi/2, \beta = \beta_0$ where the value of β_0 has to be chosen by later considerations. Thus

$$\lambda(\alpha, \beta) = \cos^{-1}[\sin\alpha \cos(\beta - \beta_0)]. \tag{27}$$

The function $D(\theta, \phi, \alpha, \beta) = G(\theta, \phi)/I(\alpha, \beta)$ is still a separable function of (θ, ϕ) and (α, β).

The initial conditions along $y = 0$ are, as before, of form

$$\alpha = \theta = \pi/2, \qquad \phi = x, \qquad \beta = f(x),$$

where $\pi/3 \leq x \leq 2\pi/3$ and

$$\mathrm{d}f/\mathrm{d}x = (D(\pi/2, x, \pi/2, f(x)))^{1/2}. \tag{28}$$

We take $\beta_0 = f(\pi/2)$ so that the direction of maximum feed illumination corresponds to the direction of maximum reflected field. The required integration of (28) using

(25)–(27) is

$$\int_{\beta_0}^{f} \frac{\mathrm{d}f}{1+\frac{9}{16}(f-\beta_0)^2} = \int_{\pi/2}^{x} \frac{4\sin x}{\cosh(6\cos x)}\,\mathrm{d}x,$$

that is

$$\tan^{-1}[\tfrac{3}{4}(f-\beta_0)] = \tfrac{1}{4}\pi - \tan^{-1}[\exp(6\cos x)].$$

It follows that

$$f-\beta_0 = \frac{4}{3}\left(\frac{1-\exp(6\cos x)}{1+\exp(6\cos x)}\right) = -\tfrac{4}{3}\tanh(3\cos x).$$

Now we choose β_0 in $(0, -\pi/2)$ so that $0<x-f(x)<\pi$ over $x\in(\pi/2, 2\pi/3)$ to prevent source blockage. This condition implies that $0{\cdot}16<-\beta_0<0{\cdot}89$. We take $\beta_0=-\pi/4$ and hence

$$f = -\tfrac{1}{4}\pi - \tfrac{4}{3}\tanh(3\cos x). \tag{29}$$

Substituting (29) into (8) we obtain

$$\tau(x) = 4\int_{\pi/2}^{x} \sin u\,\operatorname{sech}^2(3\cos u)\cot[\tfrac{1}{2}u + \tfrac{1}{8}\pi + \tfrac{2}{3}\tanh(3\cos u)]\,\mathrm{d}u$$

which is evaluated numerically over the required range of x.

From the results of the integration for $\alpha, \beta, \theta, \phi$ it is evident from figure 6 that the contours of constant G contain a larger solid angle in the (α, β) plane than was obtained in the case of model 3. This is to be expected since from Westcott and Norris (1975) $D=|\mathrm{d}\Omega'/\mathrm{d}\Omega|$ where $\mathrm{d}\Omega, \mathrm{d}\Omega'$ represent elementary solid angles of reflected ray cones and incident ray cones respectively. Now D is increased relative to model 3 due to the feed pattern taper $I(\alpha, \beta)$ illustrated by figure 7, so that for a given $\mathrm{d}\Omega$ it follows that $\mathrm{d}\Omega'$ must be increased. The -9 dB G contour includes an elliptical region extending to over 55° in the α direction and 100° in the β direction.

The reflector surface integration produces the cross sections of figure 8.

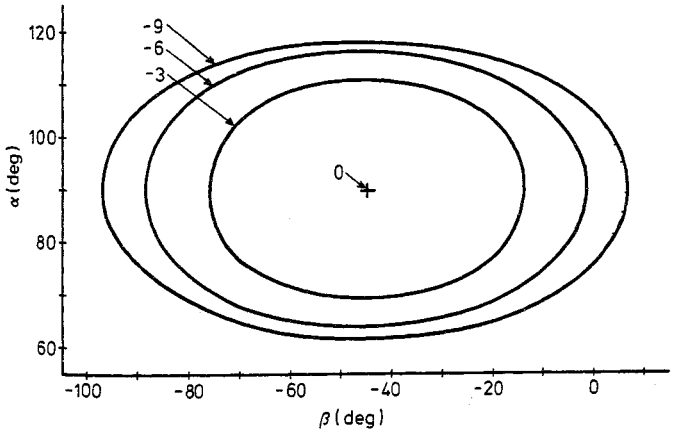

Figure 6. Constant G contours (labelled in decibels) against incident ray direction for model 4.

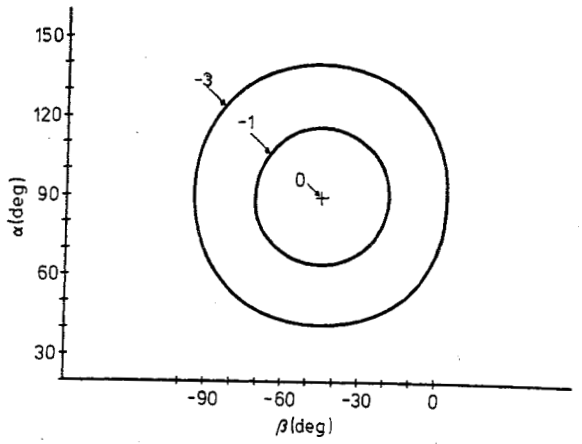

Figure 7. Constant I contours (labelled in decibels) against incident ray direction for model 4.

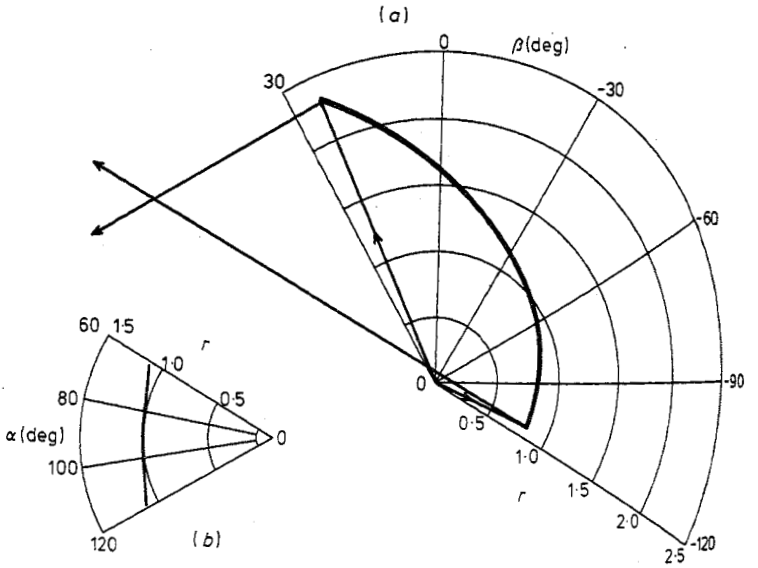

Figure 8. Reflector cross sections for model 4: (a) in $\alpha = \pi/2$ plane showing edge rays; (b) in $\beta = -\pi/4$ plane.

7. Conclusions

The synthesis of reflector surfaces for two-variable beam shaping under the geometrical-optics approximation has been considered numerically for the hyperbolic form of the governing equations.

Theoretical formulae given in a previous paper by the authors have been developed for use on a computer. First- and second-order finite-difference approximations for the partial differential equations have been derived and tested numerically against exact solutions and very good accuracy in the computed results has been obtained.

The procedure was also applied to two more practical models. In these the two-variable far-field beam shape has the same prescribed elliptical variation but in one model the source illumination is isotropic and in the second model it is tapered. In both cases reflector surfaces with zero source blockage have been generated successfully indicating that: (i) the method for setting the initial data was reasonable; and (ii) the solution extended far enough from the initial line to admit a viable reflector design.

Further work is necessary to seek any limitation which more sophisticated far-field and source field variations may impose on the design method. Since the method is based on power distributions only (no far-field phase specification) it is particularly advantageous to the microwave antenna designer provided the resultant design is tested using diffraction theory in the usual way. A possible application is to the design of satellite antennae used to cover specified areas on the surface of the earth.

References

Brickell F and Westcott B S 1976 *J. Phys. A: Math. Gen.* **9** 113–28

Courant R and Hilbert D 1962 *Methods of Mathematical Physics* vol 2 (New York: Interscience) pp 476–8

Forsythe G E and Wasow W R 1960 *Finite-Difference Methods for Partial Differential Equations* (New York: Wiley) § 7

Mitchell A R 1969 *Computational Methods in Partial Differential Equations* (London: Wiley) chap 4

Westcott B S and Norris A P 1975 *J. Phys. A: Math. Gen.* **8** 521–32